1. Background information and service history

Metallic assemblies exhibit lower service-life when operated at elevated temperatures. Depending on the particular environmental and loading conditions, the most common causes of elevated-temperature failure can be classified as creep-originated, environmentally induced, high-temperature fatigue and thermal fatigue [1].

The present study focuses on the investigation of the systematic short-time failure of a superheater pipeline, part of the main heat exchanger assembly operating with steam, in a power-plant unit in Northern Greece. The multi-curved pipeline was constructed over a lignite combustor, 30 years ago. According to the original design, the whole pipeline consists of an array of individual tubes of outer diameter 38 mm, wall thickness 6 mm and length 4 m. These tubes are properly welded to form a pipeline with a total heat exchange area of 5200 m^2. The suggested construction materials were the steel grades: 15Mo3, 13MoCr44 and 10CrMo910 (Table 1), commonly proposed for the production of pressure vessels.

The average steam velocity along the pipeline was 9.1 $m\,s^{-1}$ and the steam outlet flow rate 893 $t\,h^{-1}$. The operating conditions of the pipeline are summarised in Table 2.

An increased need for maintenance operations has been observed over the past several years, reaching eventually an average time period of 15 days of continuous operation. Such a high frequency introduces a costly procedure for the plant operation due to the plant downtime required for the repair/replacement of the failed pipeline parts. In the particular case, all the main elevated-temperature failure mechanisms are equally possible:

- Creep, due to the deviation between the designed and the actual operating conditions (abnormal operation).
- Environmentally induced failure, due to the effect of the combustion gases, the chemical composition of which can be diversified according to the lignite's mineralogical structure that can be crucially varied with the depth of the exploitation field.

Table 1
Chemical composition of the suggested steel grades (wt%)

Steel grade	W.Nr.	C	Si	Mn	*P* (max)	*S* (max)	Cr	Mo
15Mo3	1.5415	0.12–0.20	0.10–0.35	0.40–0.90	0.035	0.030	–	0.25–0.35
13CrMo44	1.7335	0.08–0.18	0.10–0.35	0.40–1.00	0.035	0.030	0.70–1.10	0.40–0.60
10CrMo910	1.7380	0.06–0.15	⩽0.50	0.40–0.70	0.035	0.030	2.00–2.50	0.90–1.10

Table 2
Designed and actual operating conditions of superheater pipeline

	Designed	Actual
Steam inlet temperature (°C)	370	449
Steam outlet temperature (°C)	443	505
Steam inlet pressure (bar)	186.7	–
Steam outlet pressure (bar)	183.2	–

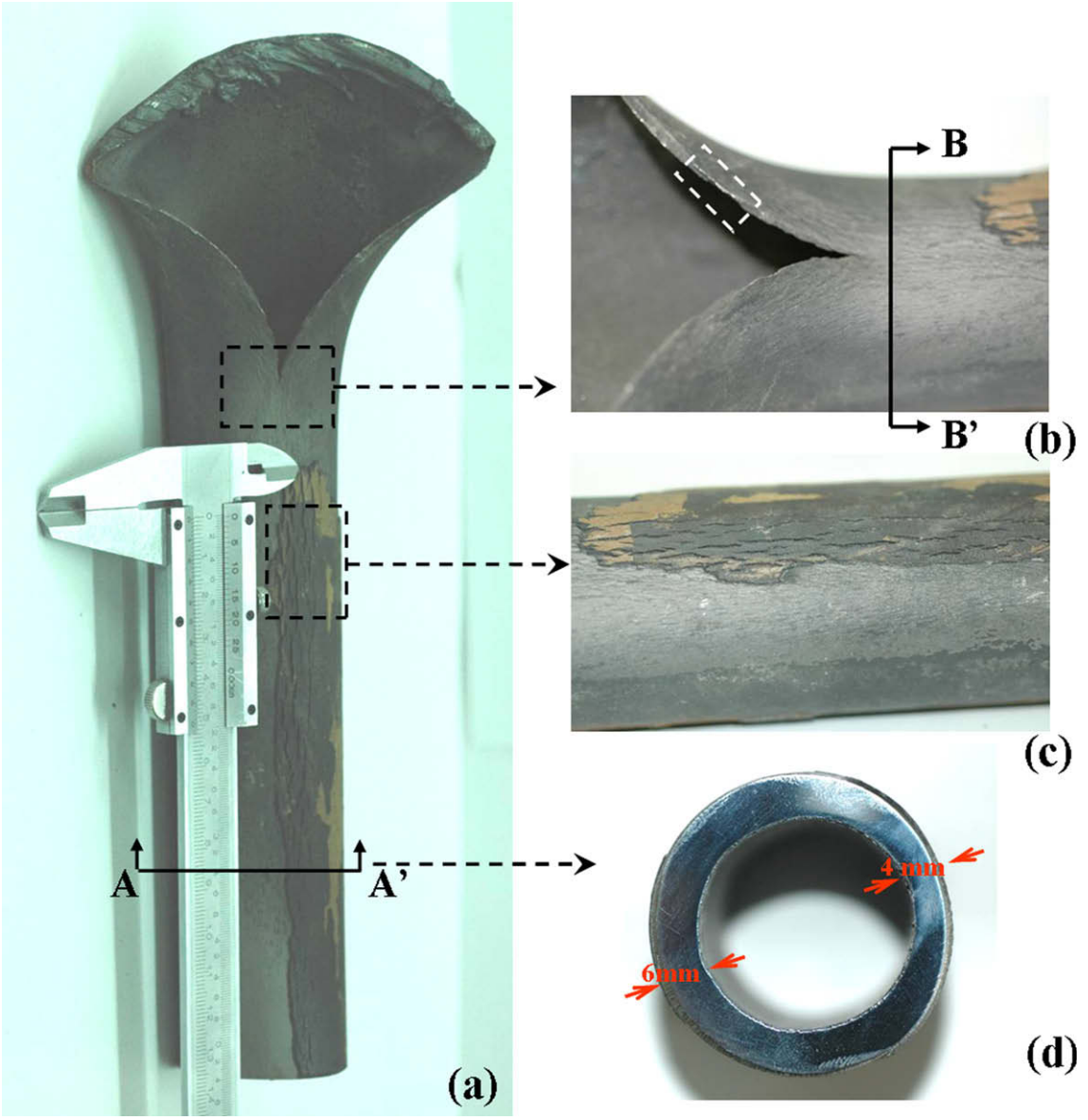

Fig. 1. Macrographs of the failed-tube retrieved from a curved area of the pipeline: (a) total view of the retrieved part, indicating "fish-mouth" rupture; (b) zooming of (a), at the area of the tip of the rupture lip; (c) zooming of (b), at the area of tube swelling and (d) cross-section ring along the line AA′ of (a).

- Thermal fatigue, due to the frequent operation interruptions for the repair of the pipeline.
- High-temperature fatigue, due to alternations of the steam pressure.

The present study is focused on a thorough metallurgical investigation of the pipeline failed parts to identify the failure mechanisms and propose a more reliable solution, leading to maximum extension of the pipeline's service-life.

2. Experimental techniques

Macroscopic observations of the failed tubes were performed with a Leica MS 5 and a Nikon SMZ 1500 stereomicroscope. In order to reveal the main failure mechanisms, microscopic observations were carried out using an FEI XL40 SFEG scanning electron microscope (SEM) equipped with an electron dispersive spectrometry X-ray microanalysis system (EDAX) for elemental analysis of selected areas. Metallographic examination was conducted using a Nikon Epiphot 300 inverted metallurgical microscope. Prior to that, cross-sections of the failed tubes were prepared using hot-mounting, wet grinding up to 1200 grit SiC paper and polishing with diamond and silica suspensions. Chemical etching was performed by immersion of the specimens in Nital reagent: 2% HNO_3 ethanol solution for 10 s, followed by cleaning with ethanol and drying with hot-air stream. Vickers hardness measurements on characteristic areas of the welded specimens were carried out using an Instron-Wolpert tester, applying a load of 10 kg [2].

3. Results

Systematic recording of data over one year of pipeline's service indicated that local material's failures were occurring with an average period of 15 days and were localised either at curved areas of the tubes, or in the neighbourhood of circumferential weldments. Microstructural investigations of failed-tube parts, representative of these two failure cases are discussed below.

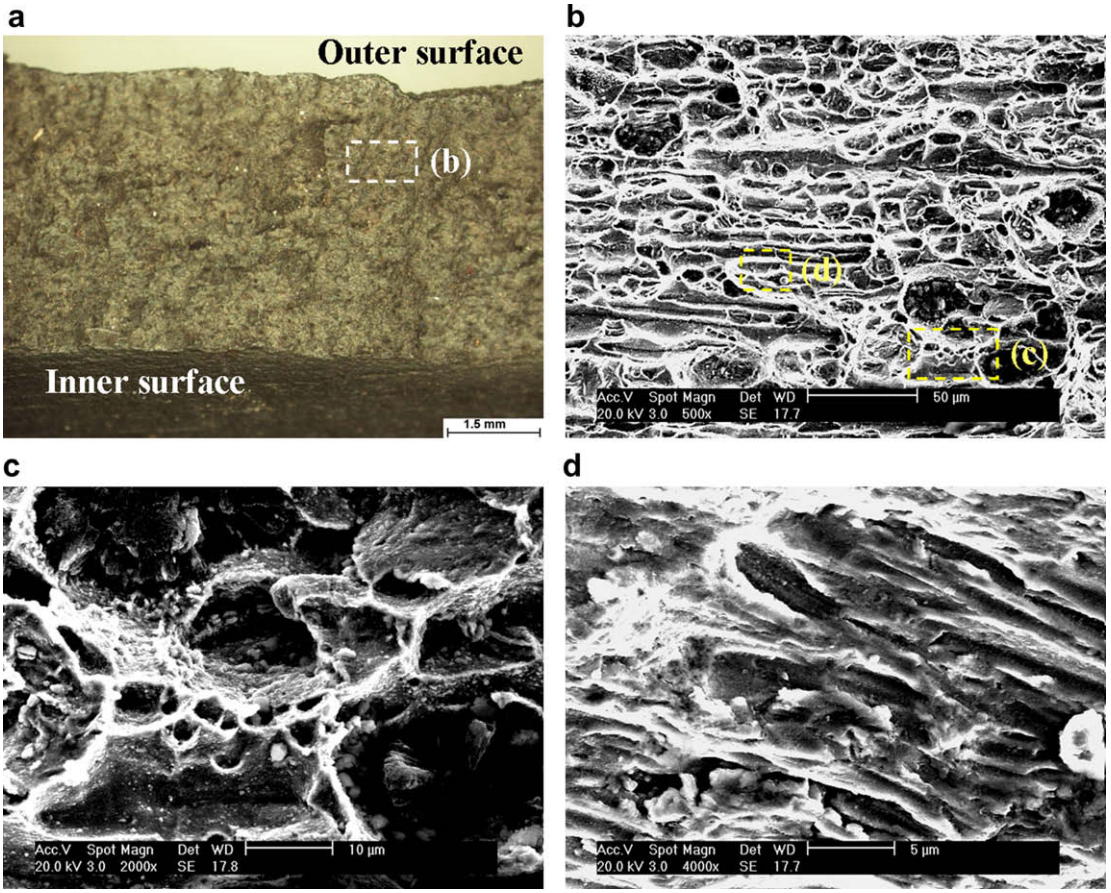

Fig. 2. Fracture surface of the rupture lips, indicated in Fig. 1a with a dashed rectangle: (a) stereo-graph of the dimpled fracture surface; (b) SEM image of the zoomed area indicated in (a); (c) SEM image of micro-voids, present on the fracture surface and (d) SEM image of dimples oriented along the initial direction of the material's grains.

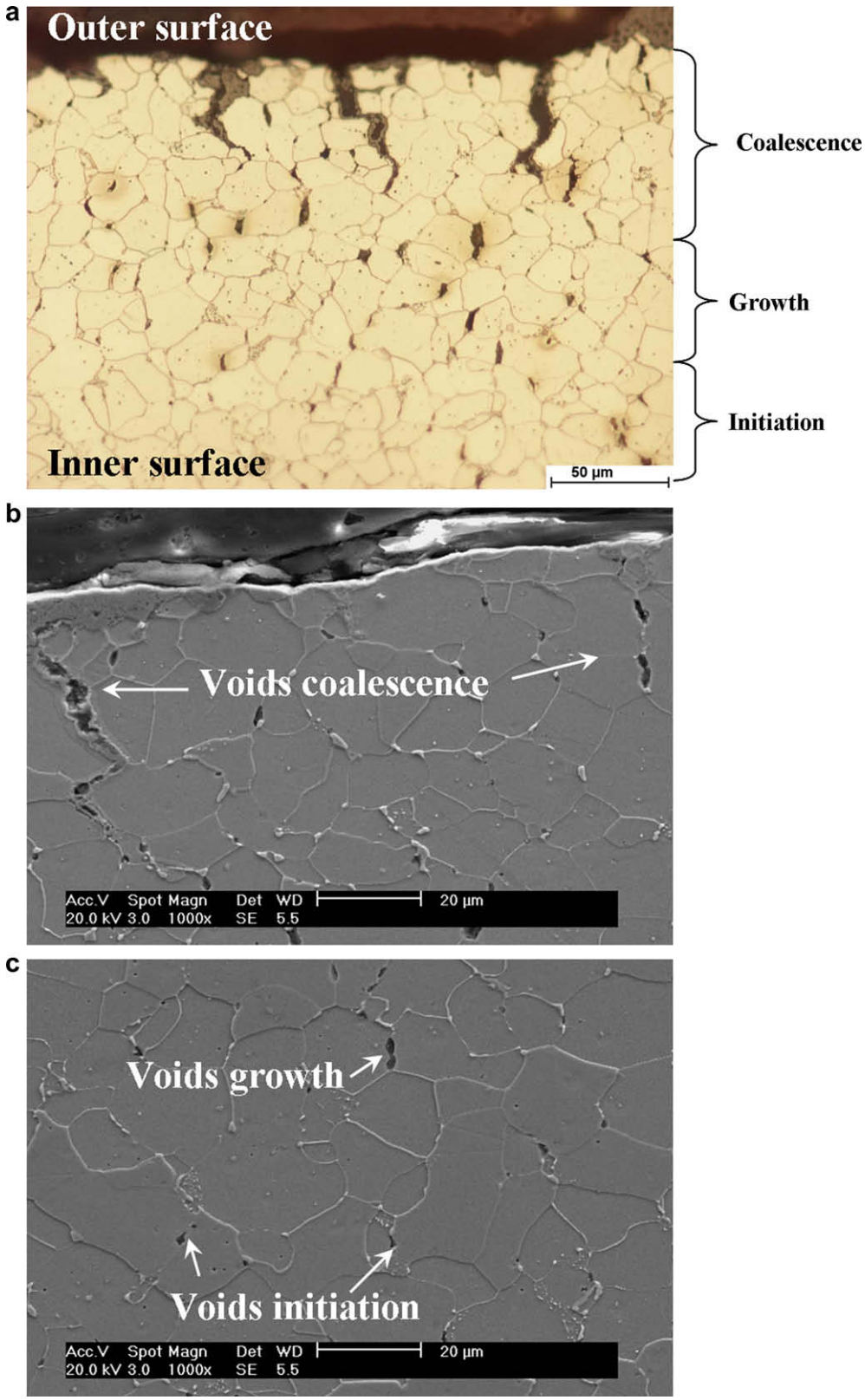

Fig. 3. Cross-sections along the line BB' of Fig. 1b: (a) optical micrograph of the failed-tube wall; (b) SEM image of outer surface of the failed-tube wall and (c) SEM image of inner surface of the failed-tube wall.

3.1. Failure at the curved areas of the pipeline

The failed parts retrieved from curved pipeline areas exhibit the typical "fish-mouth" thin-lip rupture (Fig. 1a), commonly observed in cases of creep-induced failure of superheater and reformer tubes [3,4].

In the particular case, rupture occurred always at the inner wall of the curved tube. The wall thickness at the tip of the "fish-mouth" was diminished from its original value of 6 mm down to about 1 mm, whilst the typical metal plastic flow striations could also be clearly observed along the tube axis (Fig. 1b). At a distance of about 30 mm from the rupture tip, a bump on

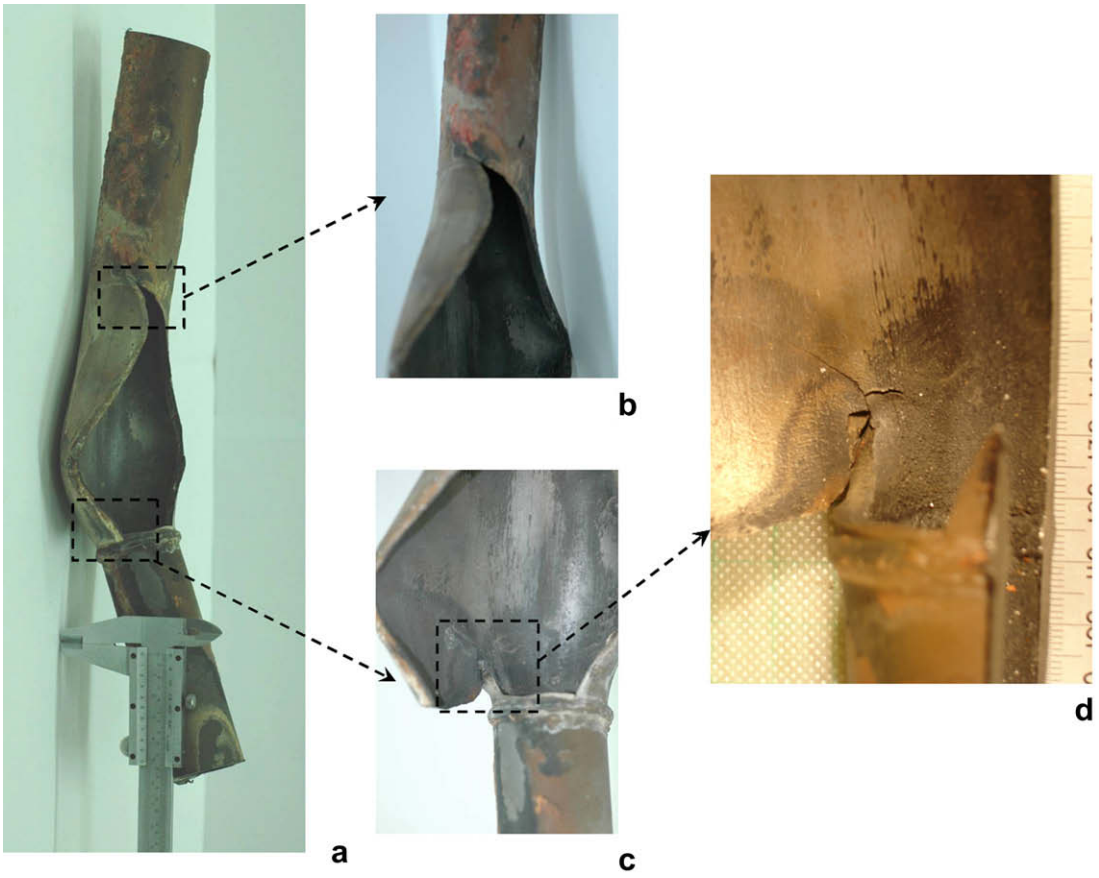

Fig. 4. Macrographs of the failed-tube retrieved from area of the pipeline with circumferential weldment: (a) total view of the retrieved part, exhibiting a "cobra" appearance and (b–d) zooming of characteristic areas, indicated in (a).

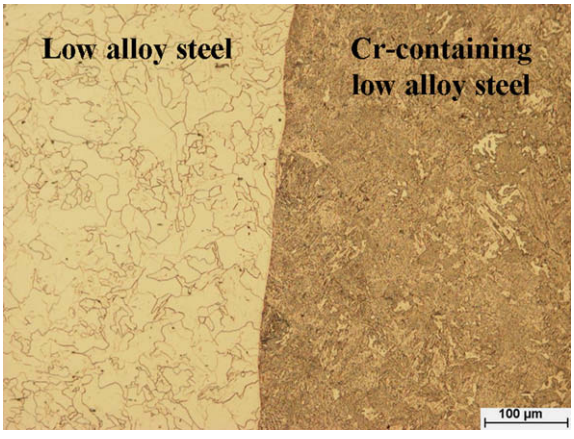

Fig. 5. Optical micrograph of a cross-section perpendicular to the circumferential weldment, revealing solid-state welding of dissimilar steel grades.

the inner wall had occurred, partially covered by a characteristic oxide layer (Fig. 1c, brown areas) exhibiting an "orange-peel" effect. On the oxide layer, yawning of intermittent secondary rupture cracks in the direction of the tube axis can be recognised. The secondary rupture cracks can be also observed as slight openings (Fig. 1c), at areas where the base metal is revealed due to

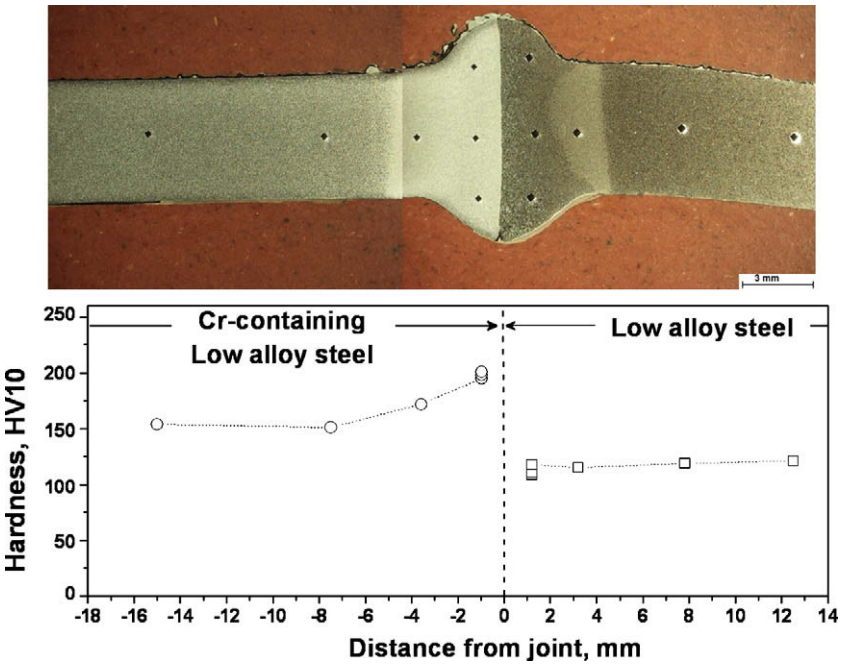

Fig. 6. Stereo-graph of a cross-section perpendicular to the circumferential weldment, areas and values of the Vickers hardness measurements performed.

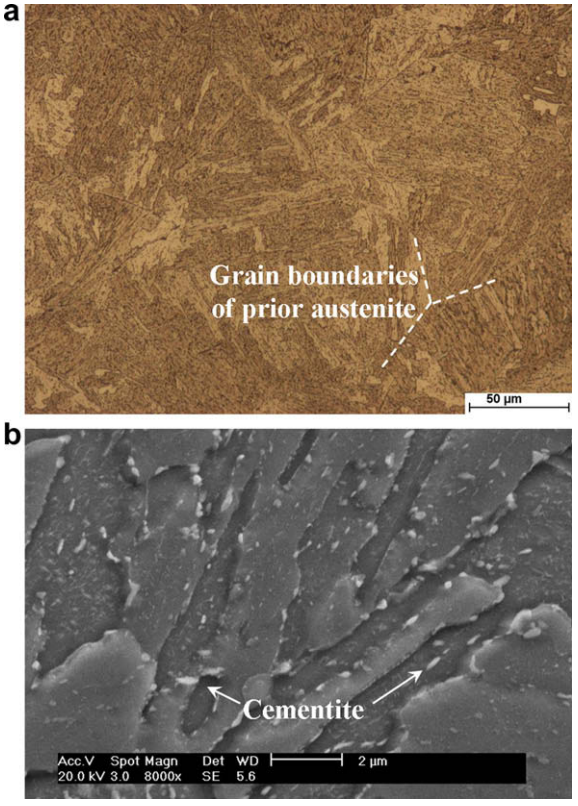

Fig. 7. Optical (a) and SEM (b) images of the Cr-containing steel grade, from cross-sections in the neighbourhood of the joint boundary.

detachment of the cracked oxide layer, most likely caused during the maintenance works. Similar features have been observed in the case of creep failure of turbine blades [5]. Such oxide layers were also present on the diametrically opposite area of the outer wall of the curved tube; however they were much thinner, free of cracks and well adhered to the parent metal. Wall thinning extending to a distance of about 120 mm from the rupture tip was observed; at this location the thickness of the inner wall was measured at 4 mm, corresponding to a 33% reduction of its original dimension (Fig. 1d).

Stereo- and SEM-photographs of the rupture-lips' (Fig. 1b, marked area) are shown in Fig. 2. On the dimpled fracture surface (Fig. 2b), two co-existing features can be clearly distinguished:

- Large equiaxial voids arising from the coalescence of creep voids of smaller dimensions (Fig. 2c).
- Elongated dimples corresponding to the initial orientation of the material's grains due to the unidirectional tube forming process (Fig. 2d).

The creep void evolution across the tube wall is presented in Fig. 3a. At the outer surface of the tube, void coalescence (Fig. 3b) resulted in intergranular surface cracks of a mean length of 50 μm, filled with oxidation products. Consequently, a second zone of creep void growth can be observed, extending from a depth of about 70 μm to about 130 μm (Fig. 3c); whilst toward the inner surface of the wall, initiation of individual voids appeared along the grain boundaries (Fig. 3c) [6,7]. The co-existence on the same tube cross-section of the three stages in creep void evolution: initiation/growth/coalescence is indicative of a temperature gradient across the wall through which heat exchange is taking place between the hot lignite combustion gases in contact with the outer surface of the tube and the high-pressure steam flow in contact with the inner surface of the tube.

The tube material identification was obtained by applying both metallographic observation and EDAX microanalysis; which showed that it was a low-alloy ferritic steel, probably corresponding to the 15Mo3 grade proposed by the designers of the pipeline. Precipitates observed at the grain boundaries (Fig. 3b and c) indicated cementite spheroidisation, due to the prolonged heating of the material during operation, at a temperature close to A_{C1}.

3.2. Failure in the neighbourhood of welding seams

The failed parts of the pipeline retrieved from areas near circumferential weldments (Fig. 4) exhibit a "cobra" appearance [3], with fracture cracks initiating near the seam (Fig. 4c) and propagating within one of the joined tubes, in a direction almost parallel to its axis (Fig. 4d).

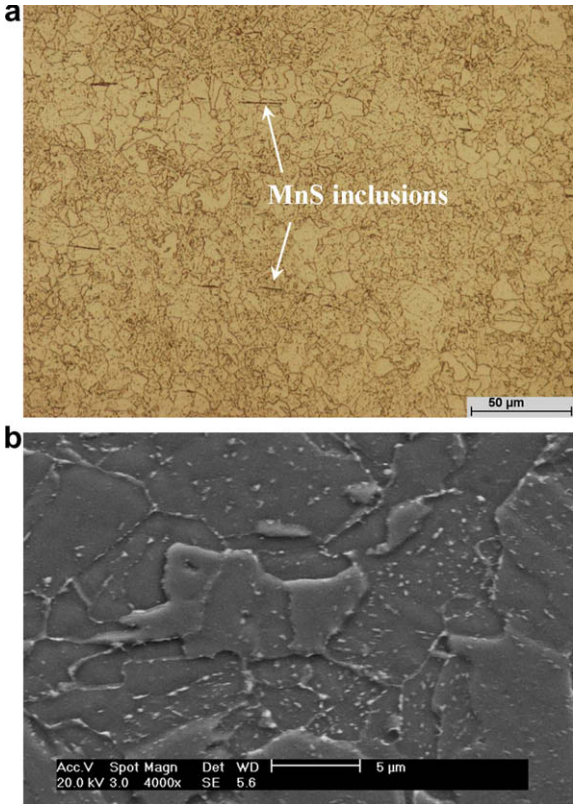

Fig. 8. Optical (a) and SEM (b) images of the Cr-containing steel grade, from cross-sections at an area of intermediate hardness.

Metallographic observations of the weldment's cross-section (Fig. 5) revealed both the materials' dissimilarity of the joined tubes, as well as the absence of fusion zone or filler material, which indicate that a high-temperature solid-state welding technique was applied. EDAX microanalysis indicated that one of the tubes was a Cr-containing steel, probably corresponding to the 13CrMo44 or 10CrMo910 grades also proposed by the designers, whilst the other one, within which fracture cracks had propagated, was a low-alloy ferritic steel, as in the previous case. Although there is a clear boundary between the two welded parts and there is no apparent metallurgical bonding between the two joined surfaces, the seam nevertheless can be characterised as one of excellent quality, since failure initiation was clearly located outside of it.

Vickers hardness measurements performed along the direction of the tube's axis (perpendicular to the seam, Fig. 6) revealed a substantial drop in hardness values between the two sides adjacent to the seam:

- In the case of Cr-containing steel grade, the area near the seam exhibited a mean hardness of 200 HV10; at a distance of 3.5 mm from it the value dropped to 170 HV10 and further away, to that of the parent material (~150 HV10).
- In the case of ferritic steel, hardness exhibited a slight increase from 110 HV10 near the seam to 120 HV10 at the parent material.

The solid-state metallurgical transformations, attributed to both the welding process as well as to the high-temperature service conditions, that led to the above hardness distribution were extensively studied by metallography and SEM observations.

In the case of Cr-containing steel grade, the area close to the joint boundary, of 2 mm width, exhibited no re-solidification features, but had the characteristic upper-bainite structure (Fig. 7), with the grain boundaries of prior austenite clearly distinguished. The adjacent area of intermediate hardness of 2.5 mm width, consisted of tempered ferrite with a fine distribution of spheroidised cementite (Fig. 8). Finally, the parent material had a microstructure of ferrite with partially spheroidised pearlite (Fig. 9). Oblong dark features within the base structure correspond to MnS inclusions, entrapped during the material production and shaped during the tube forming process.

In the case of ferritic steel, the area close to the joint boundary, of 2 mm width, presented irregular ferrite grains (Fig. 10), while dark precipitations distributed within the base microstructure corresponded to residual fluxes (Al_2O_3 and/or CaO) that were entrapped during solidification of the raw material and spheroidised due to their high surface tension. The adjacent

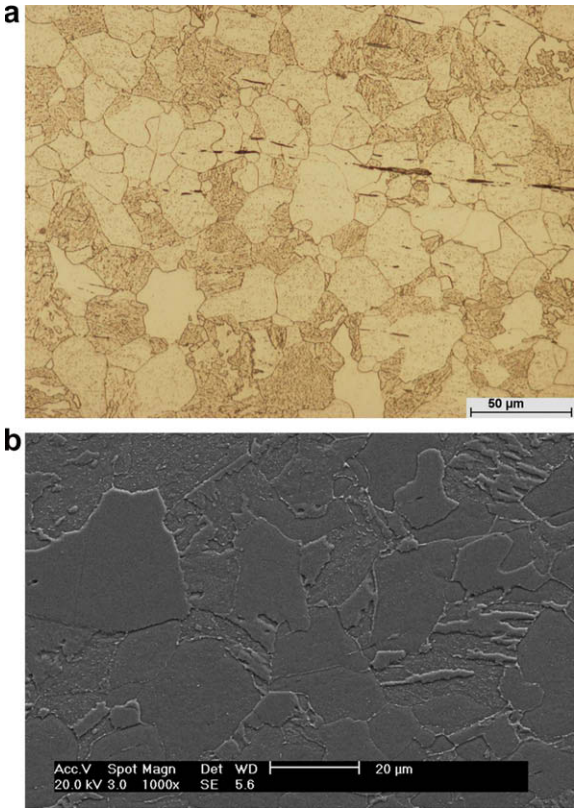

Fig. 9. Optical (a) and SEM (b) images of the Cr-containing steel grade initial structure.

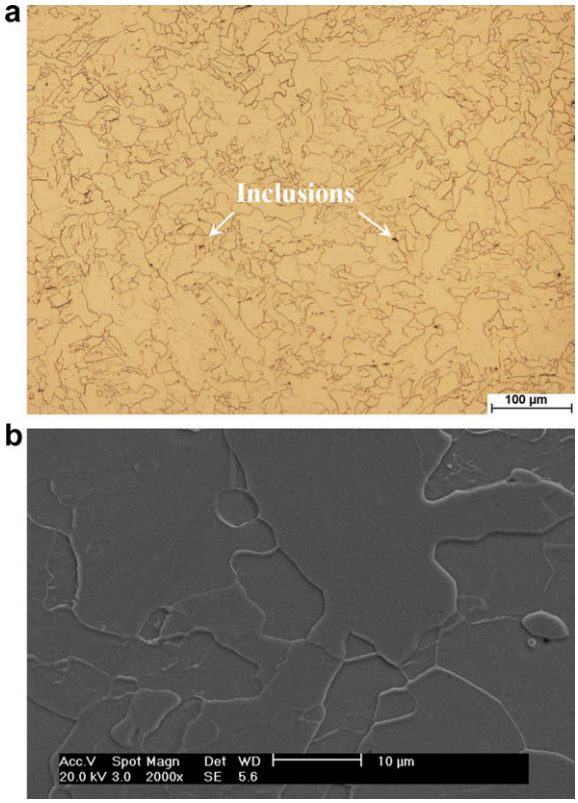

Fig. 10. Optical (a) and SEM (b) images of the ferritic steel, from cross-sections in the neighbourhood of the joint boundary.

area of 2.5 mm width also consisted of equiaxial ferrite grains, of uniform distribution, which indicates that the material was re-crystallised (Fig. 11). The carbide precipitates found at the grain boundaries probably correspond to spheroidised cementite. In the same area, individual creep voids of small size were scarcely observed. The parent structure was characterised by ferrite grains (normalised ferrite) and a high distribution of creep voids (Fig. 12).

Compared to the area of re-crystallised ferrite, the parent material exhibited large ferrite grains, of almost double the size; and round, trans-granular creep voids with an average diameter of 0.05 mm (Fig. 13a). A close view on this area revealed that the growth and coalescence of creep voids was taking place through micro-necking between two adjacent voids of crucial size (Fig. 13b). Around the voids at this area, a circular zone can be observed with clear evidence of the material dynamic re-crystallisation (Fig. 13a and b), which is attributed to ferrite straining caused during void growth.

4. Discussion and conclusions

In the present study, the metallurgical modifications taking place during high-temperature exposure of a steel pipeline that led to local material's failure were investigated. Failure was localised either at curved areas of the tubes, or in the neighbourhood of circumferential weldments and the failed parts exhibited a "fish-mouth" or a "cobra" appearance respectively, morphologies characteristic of creep rupture. The short-time service-life (~15 days of continuous operation) indicated the absence of a primary creep stage, commonly appearing in cases of operation under conditions of a high-temperature and/or high stress regime.

- Since no data on the actual steam pressure were available and considering that there was no deviation from the design, the hoop stress was estimated at 50.5–51.5 MPa, via the Lamé equation valid for thick-wall tubes.
- The initial design of the pipeline has taken into account that steam inlet and outlet temperature were respectively 35.5% and 39.6% of the material's melting point; whilst during service these parameters were higher: 39.9% and 43.0%.
- In both failure cases presented above, rupture always took place within low-alloy ferritic steel, probably corresponding to 13Mo3 grade; whilst the presence of impurities like oblong MnS and round Al_2O_3, CaO did not seem to affect the creep behaviour of the material.

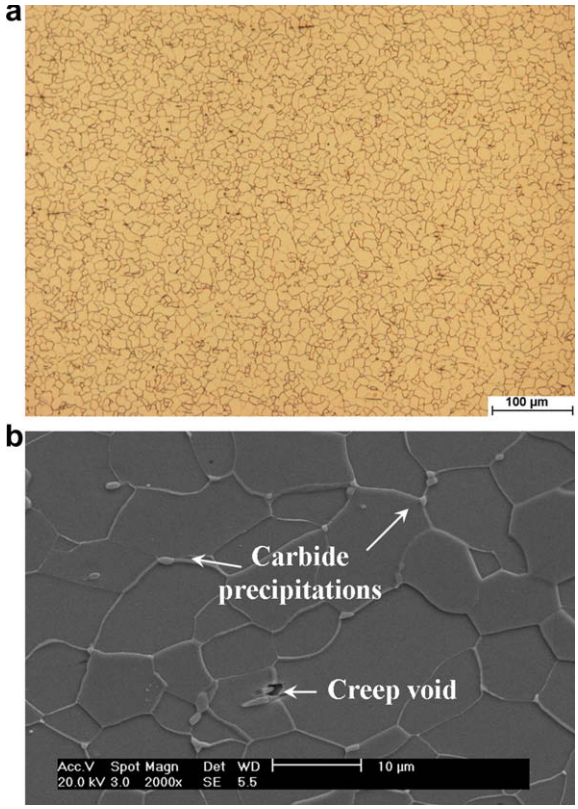

Fig. 11. Optical (a) and SEM (b) images of the ferritic steel, revealing material's re-crystallisation.

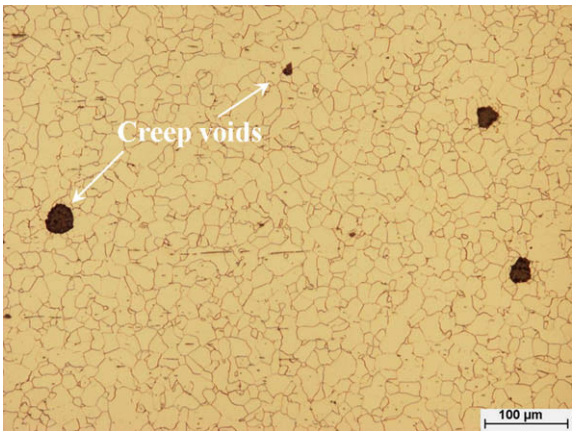

Fig. 12. Optical micrograph of initial structure of the ferritic steel.

Based on these points, the continuous pipeline review and re-design is suggested taking into account each time the calorific value of lignite that is fed to the combustion chamber of the unit. As this seems to be higher with increasing exploitation depth, the 13Mo3 grade should be rejected and more heat-resistant steel grades should be considered as materials of choice.

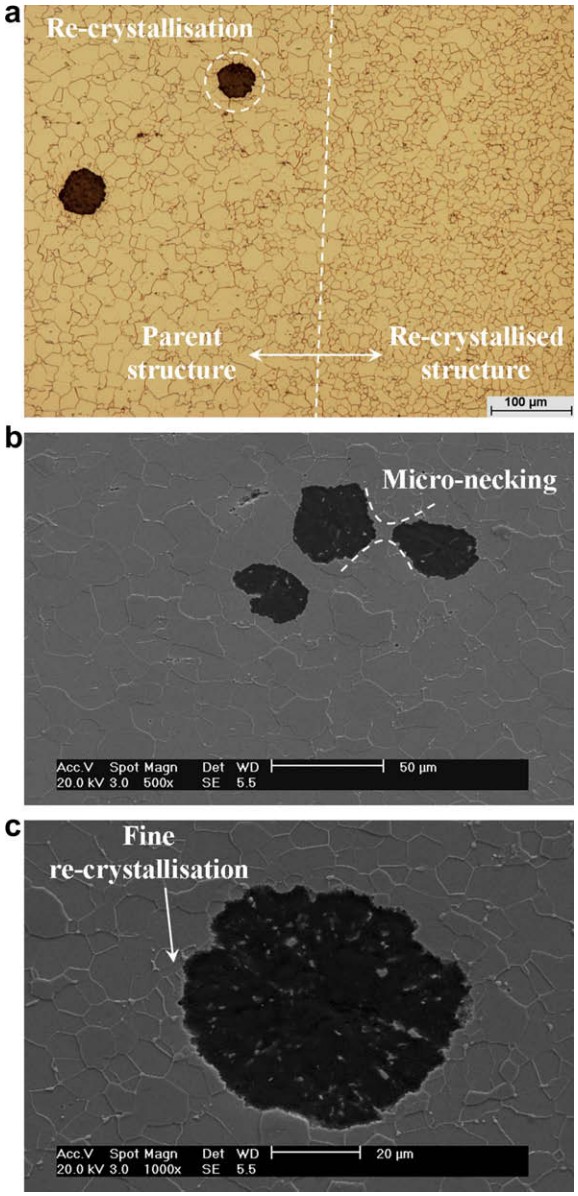

Fig. 13. (a) Optical micrograph of the boundary of the re-crystallised/initial structure of the low-alloy steel grade; (b) SEM micrograph of the parent material, indicating micro-necking between adjacent creep void and (c) SEM micrograph of the parent material, indicating fine dynamic re-crystallisation around a creep void.